Journal of Photochemistry & Photobiology A: Chemistry 392 (2020) 112348

Contents lists available at ScienceDirect

Journal of Photochemistry & Photobiology A: Chemistry

journal homepage: www.elsevier.com/locate/jphotochem

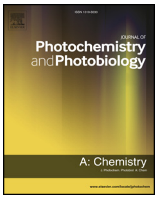

A new multifunctional sensor for sequential recognizing of Zn^{2+} and PPi in acetonitrile solution and detection of In^{3+} in DMF solution

Yuankang Xu[a], Shufang Yuan[b,*], Yanxia Zhang[a], Hanyu Wang[a], Xiaofeng Yang[a], Meishan Pei[a], Guangyou Zhang[a,*]

[a] *School of Chemistry and Chemical Engineering, University of Jinan, Jinan 250022, China*
[b] *Henan Sanmenxia Aoke Chemical Industry Co. Ltd., Sanmenxia 472000, China*

ARTICLE INFO

Keywords:
Schiff base
In^{3+}
Zn^{2+}
Multifunction sensor
Gaussian calculations
Real water samples

ABSTRACT

A simple multifunctional sensor, **X**, was designed and synthesized based on 8-hydroxy-2,3,6,7-tetrahydro-1H,5H-pyrido[3,2,1-ij]quinoline-9-carbaldehyde and imidazo[2,1-b]thiazole, which could sequentially identify Zn^{2+} and PPi in acetonitrile buffer solution through the presence or absence of fluorescent signals and could detect In^{3+} in DMF buffer solution with obvious fluorescence enhancement. The detection limit for Zn^{2+}, PPi and In^{3+} were calculated to be 4.58×10^{-8} M, 1.07×10^{-8} M and 2.9×10^{-8} M, respectively. Moreover, **X** could quantitatively detect Zn^{2+}, PPi and In^{3+} in real water samples with the satisfactory recovery rate (90.1 %–97.6 %) and RSD (0.86 %–3.09 %). In addition, the complexation ratio between **X** and metal ions (Zn^{2+} and In^{3+}) was 1:1, which was proved by mass spectrometry titration. The binding mode and sensing mechanism of **X** to metal ions (Zn^{2+} and In^{3+}) were verified by Gaussian calculation based on B3LYP/6-31 G(d) and B3LYP/LanL2DZ basis set.

1. Introduction

As we all known, metal ions and anions play a vital role in many fields of medicine, industry, chemistry and biology [1–4]. Among the various metal ions, Zinc is the second most abundant transition metal ions in the human body about 2 g which are found in bones, muscles and blood [5,6]. As an essential metal element to various functions of the human body it plays an important role in many physiological processes, including gene transfection, immunologic function cellular metabolism and so on [7,8]. Also, as a vital metal element for the human health its imbalance will cause a variety of diseases such as Parkinson's disease, anorexia, nanism etc. [9,10]. indium, one of the elements of IIIA, is a shiny and soft metal and widely used in industry fields like semiconductor devices, electrode material and gas sensors [11]. Moreover, further research on indium has revealed that it is extremely toxic to lung and interfere with the metabolism of irons in the cells [12–14]. Otherwise, among the various anions, pyrophosphate (PPi, $P_2O_7{}^{4-}$), is of particular concern, because it plays an important role in a number of biological processes such as DNA and RNA polymerizations, cellular ATP hydrolysis and so on [15–19]. Therefore, it is particularly meaningful for the detection of Zn^{2+}, In^{3+} and PPi in ecosystems and biological systems.

In recent years, fluorescent sensor with low cost, simple operation and short response time have gradually replaced the traditional detection method and is becoming a new commonly used technology to detect target metal ions [20–22]. However, there are still many challenges in the research of fluorescent sensor [23]. For example, it is still a huge challenge for detection of metal ions selectively without interference of other transition metal ions with similar chemical properties, such as Zn^{2+} and Cd^{2+} or In^{3+} and Al^{3+}/Ga^{3+} [11,24–26]. Moreover, high sensitivity is another important indicator of sensors [27,28]. The detection limit of most sensors for target ions has been reported to be about 10^{-7} M, which still need to be improved to meet the practical application requirements. [12,29–31]. In addition, good solubility and adaptability, high quantum yield and wide wavelength are also the characteristics of a sensor with excellent performance [13,32–34]. So, the design and synthesis of fluorescent sensor with high sensitivity and selectivity for target ions still remains great challenging.

In a general way, compare with other types of sensors, schiff base formed from the condensation of amines and aldehydes are often designed and synthesized for detection of metal ions due to their simple structure, good solubility and high recognition of metal ions [14,35–40]. Among various aldehydes, 8-hydroxy-2,3,6,7-tetrahydro-1H,5H-pyrido[3,2,1-ij]quinoline-9-carbaldehyde contains julolidine

---

* Corresponding authors.
E-mail addresses: yuansfsales@aokechem.cn (S. Yuan), chm_zhanggy@ujn.edu.cn (G. Zhang).

https://doi.org/10.1016/j.jphotochem.2019.112348
Received 19 November 2019; Received in revised form 15 December 2019; Accepted 27 December 2019

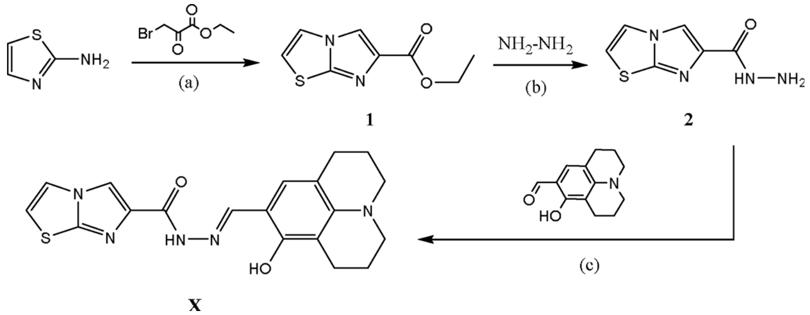

X

Scheme 1. Synthesis routes of **X**. Conditions: (a) THF/ethanol, r.t./refluxed, 20 h/4 h; (b) ethanol, r.t., overnight; (c) ethanol, r.t., TsOH, 48 h.

moiety, which is often used to synthesize schiff base because of their water solubility, good planarity and structural rigidity [41,42]. Meanwhile, heterocyclic azoles, containing imidazole and thiazole ring, are important active molecules that can provide N or S as donor atoms to bind metal ions [43,44]. The study of schiff base with heterocyclic and julolidine structures is of great value and should be paid more attention. Obviously, most of the sensors that have been reported are single-ion responsive, and a few are capable of detecting multiple targets in respective systems [45–48]. Multi-objective detection of metal ions can better reflect the diversity of the properties of a sensor, which should be valued and favored.

In this work, a new schiff base, **X**, was designed and synthesized by a simple condensation of 8-hydroxy-2,3,6,7-tetrahydro-1H,5H-pyrido [3,2,1-ij]quinoline-9-carbaldehyde and imidazo[2,1-b]thiazole-6-carbohydrazide. As expected, **X** could be used as a multifunctional sensor with high sensitivity and selectivity for sequential detection of Zn^{2+} and PPi in acetonitrile buffer solution and for cyclic detection of In^{3+} in DMF buffer solution.

2. Experimental section

2.1. General methods

All reagents and solvents in this project were of analytical grade and were used without any treatment. The counter anions of all metal ions are chloride, sulfate or nitrate ions. All anionic solutions are corresponding sodium or potassium solutions. The Stock solutions of the ions (0.03 M) were prepared by distilled water and tap water. The stock solution of **X** (1×10^{-5} M) was prepared in acetonitrile/H_2O and DMF/H_2O at 25 °C. The fluorescence spectral and UV–vis spectra were obtained by Edinburgh Instruments Ltd-FLS920 Fluorescence Spectrophotometer and Shimadzu 3100 spectrometer. ^{1}H NMR and ^{13}C NMR measurement was performed on a Bruker AV III NMR spectrometer with tatramethysilane (TMS) as internal standard and DMSO as solvent at 400 and 100 MHz, respectively. Infrared spectral data was obtained on a Bruker Vertex 70 FT-IR spectrometer using samples as KBr pellets. The sensing mechanism of **X** to metal ions (Zn^{2+} and In^{3+}) were examined by Density functional theory (DFT) calculation which carried out by Gaussian 09 program based on B3LYP/6-31 G(d) and B3LYP/LanL2DZ basis set [48].

2.2. Synthesis of X

Compound **1** and **2** were synthesized according to the previous reported reference [49]. Synthesis of (E)-**N'-((8-hydroxy-2,3,6,7-tetrahydro-1H,5H-pyrido [3,2,1-ij] quinolin-9-yl)methylene)**imidazo [2,1-b]thiazole-**6-carbohydrazide** (**X**). imidazo[2,1-b]thiazole-6-carbohydrazide (compound **2**, 161 mg, 0.884 mmol) and 8-hydroxy-2,3,6,7-tetrahydro-1H,5H-pyrido[3,2,1-ij]quinoline-9-carbaldehyde (210 mg, 0.967 mmol) were mixed in 10 ml of ethanol. Then, 2 mg of TsOH (4-methylbenzenesulfonic acid) as a catalyst were added to the above reaction mixture. After that, the mixture was stirred for 48 h at room temperature until the orange precipitate appeared. After the reaction, the orange precipitate was collected by filtration and washed with cold ethanol to obtain the pure orange solid **X**. Yield: 141 mg, 41.9 %. Ms (ESI): m/z = 382.14 $[M+H]^+$, 404.12 $[M + Na]^+$. FTIR (KBr, cm^{-1}): 3312 (N-H), 1673 (C = O), 1673 (C = N). ^{1}H NMR (400 MHz, DMSO) δ 12.03 (s, 1 H), 8.63 (s, 1 H), 8.55 (s, 1 H), 8.20 (d, J = 4.5 Hz, 1 H), 7.64 (d, J = 4.5 Hz, 1 H), 6.86 (s, 1 H), 3.38 (dd, J = 10.7, 5.1 Hz, 4 H), 2.85 – 2.77 (m, 4 H), 2.07 (dt, J = 11.2, 5.6 Hz, 4 H). ^{13}C NMR (101 MHz, DMSO) δ 157.73, 155.08, 151.27, 145.60, 140.81, 128.57, 125.97, 120.72, 116.72, 115.89, 112.88, 106.81, 106.43, 49.80, 49.34, 26.95, 22.00, 21.18, 20.69.

3. Results and discussion

As shown in scheme 1 , **X** was designed and synthesized in medium yield according to the synthetic route. Compound **1** (ethyl imidazo[2,1-b]thiazole-6-carboxylate) and compound **2** (imidazo[2,1-b]thiazole-6-carbohydrazide) were synthesized according to a previous report. Then, **X** was synthesized by the reaction of Compound **1** and **2** with 41.9 % yield in ethanol and characterized by ^{1}H NMR (Fig. S1), ^{13}C NMR (Fig. S2), FTIR (Fig. S3), ESI-MS (Fig. S4). All of the data in the spectra were in whole accordance with the structure.

3.1. The spectroscopic studies of X toward Zn^{2+} and $P_2O_7^{4-}$ in acetonitrile buffer solution

The fluorescence sensing properties of **X** toward various metal ions (Zn^{2+}, Ag^+, Cr^{3+}, Mg^{2+}, In^{3+}, Al^{3+}, Co^{2+}, Cu^{2+}, Ga^{3+}, K^+, Li^{2+}, Cd^{2+}, Mn^{2+}, Hg^{2+}, Ni^{2+} and Fe^{3+}) were explored in acetonitrile/buffer solution (v/v = 9/1, tris = 10 mM, pH = 7.4). As shown in Fig. 1(a) and (b), the fluorescence intensity of **X** was weak under excitation wavelength of 365 nm, which was significantly enhanced (about 12 times) at 491 nm when Zn^{2+} was added, while the fluorescence intensity did not change in the presence of other metal ions [50]. Furthermore, fluorescence pictures of a solution of **X** in the absence and presence of various metal ions under UV light were shown in Fig. 1(c). Consistent with the fluorescence spectrum change, the color of the solution was weak when no metal ions were present, had significant change from colorless (Φ = 0.02) to bright yellow-green (Φ = 0.26) when Zn^{2+} were added, demonstrating that **X** could be used as a sensor for Zn^{2+}. The UV–vis spectral studies of **X** toward various metal ions were also shown in Fig. S5. Zn^{2+}, Co^{2+}, Cu^{2+}, Mn^{2+} and Ni^{2+} could cause significant changed in the UV spectrum, which mean that they could form complexes with **X**. However, after complexing with **X**, their optical phenomena under ultraviolet lamp were different. Furthermore, competition experiments were also shown in Fig. S6. The presence of Co^{2+} and Cu^{2+} could interfere with the specific recognition of Zn^{2+} by **X** [51,52]. These results indicated that **X** could be used as a sensor for Zn^{2+} even in the presence of most metal ions.

To further explore the sensing properties of **X** toward Zn^{2+}, the fluorescence and absorption titration spectral were carried out in acetonitrile/buffer solution (v/v = 9/1, tris = 10 mM, pH = 7.4). As

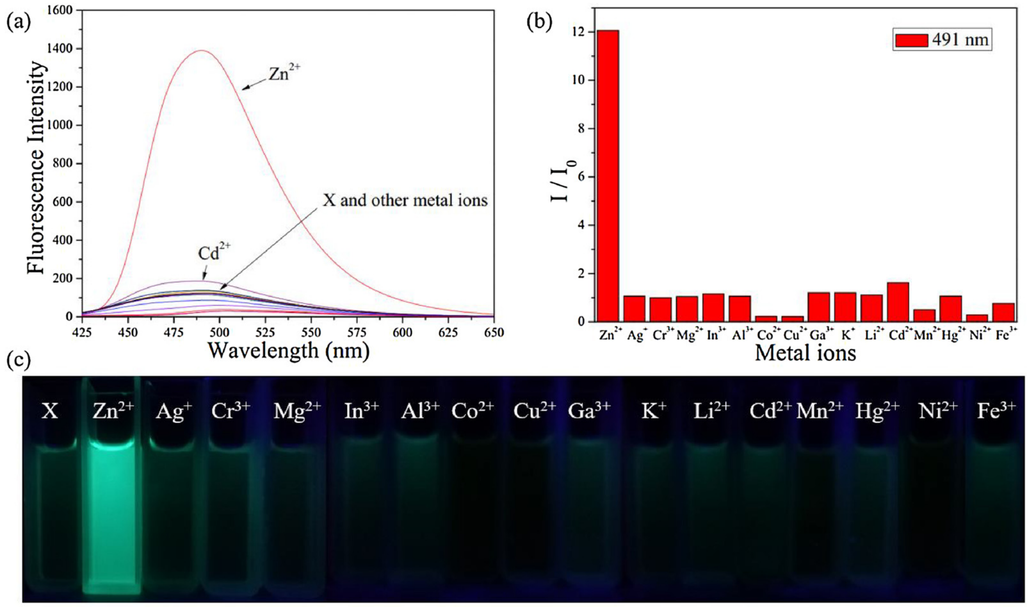

Fig. 1. (a) and (b) Fluorescence spectral changes of **X** (1×10^{-5} M) upon the addition of various metal ions (Zn^{2+}, Ag^{+}, Cr^{3+}, Mg^{2+}, In^{3+}, Al^{3+}, Co^{2+}, Cu^{2+}, Ga^{3+}, K^{+}, Li^{2+}, Cd^{2+}, Mn^{2+}, Hg^{2+}, Ni^{2+} and Fe^{3+}) in acetonitrile/buffer solution (v/v = 9/1, tris =10 mM, pH = 7.4). (c) Fluorescence pictures of a solution of **X** in the presence of various metal ions under UV light.

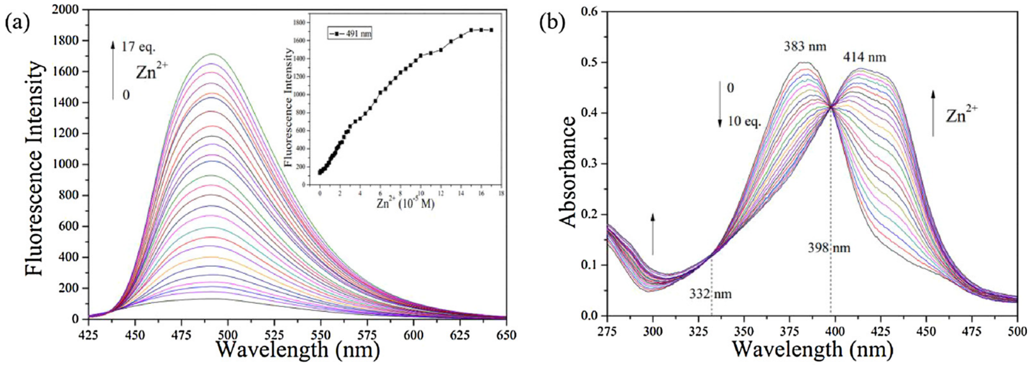

Fig. 2. (a) and (b) Fluorescence and absorption titration spectral of **X** (1×10^{-5} M) upon the addition of different concentrations of Zn^{2+} in acetonitrile/buffer solution (v/v = 9/1, tris =10 mM, pH = 7.4). Fig. 2(a) inset: the change of fluorescence intensity of **X** with the addition of Zn^{2+}.

shown in Fig. 2(a), the **X** displayed a weak fluorescence intensity under excitation wavelength of 365 nm. The fluorescence intensity of **X** increased gradually with the increased of Zn^{2+} concentration from 0 to 15 equiv. and reached a plateau at 491 nm (Fig. 2(a) inset). As shown in Fig. 2(b), the absorption band of free **X** centered at 383 nm. Upon gradually addition of Zn^{2+} to **X** from 0 to 10 equiv., the absorption band at 383 nm decreased gradually, while the absorption band near 414 nm and 300 nm increased gradually with two clear isosbestic points at 332 nm and 398 nm, suggesting that the **X** could form stable complexes (**X**[Zn^{2+}]) with Zn^{2+}. In addition, on the basis of titration experimental data, the detection limit and the association constant of **X** for Zn^{2+} were calculated to be 4.58×10^{-8} M and 1.02×10^{4} M^{-1}, respectively, according to the formula LOD = 3σ/s (Fig. S7) and the Benesi-Hildebrand eqn (2) (Fig. S8).

The effect of pH on **X** performance was measured in the pH range 2–12. As shown in Fig. S9, the **X** had no fluorescence in the pH range of 2–12. However, in the presence of Zn^{2+} (10 equiv.), the fluorescence intensity of **X** was weak and stable in the pH range of 2–6, gradually increased in the pH range of 6–8 and remained basically unchanged in the pH range of 8–12, indicating that **X** could be used as a sensor to detect Zn^{2+} at pH range of 7.4–10.

Moreover, the fluorescence sensing properties of **X**[Zn^{2+}] toward various anions ($Na_4P_2O_7$, $NaNO_3$, NaS_2O_3, $NaHSO_3$, NaBr, NaCl, $NaNO_2$, Na_2CrO_4, NaF, $NaBF_4$, Na_2S, Na_2SO_4, $NaHCO_3$ and KI) were also explored in acetonitrile/buffer solution (v/v = 9/1, tris =10 mM, pH = 7.4). As mentioned above, the fluorescence intensity of **X** was significantly enhanced when Zn^{2+} were added. So that, as shown in Fig. 3(a), the **X**[Zn^{2+}] had a moderate fluorescence under excitation wavelength of 365 nm. When various anions were added to the solution of **X**[Zn^{2+}], only PPi could cause significant changed (Fig. S10) in fluorescence intensity due to its ability to extract Zn^{2+} from the **X**[Zn^{2+}] and cause the **X** to be dissociated, while other anions did not. Moreover, as shown in Fig. 3(b), the **X**[Zn^{2+}] could still detect PPi in the presence of other anions. In addition, it could be clearly seen from Fig. 3(c) that the fluorescence intensity of **X**[Zn^{2+}] at 491 nm gradually decreased with the cumulative addition of PPi from 0 to 10 equiv. (Fig. 3(c) inset). On the basis of titration experimental data, the relevant parameters were also calculated, including the detection limit of **X**[Zn^{2+}] on PPi and the association constant of **X**[Zn^{2+}] with PPi, which were 1.07×10^{-8} M and 5.7×10^{4} M^{-1}, respectively, based on the above methods (Fig. S11 and Fig. S12). Finally, as shown in Fig. 3(d), the fluorescence intensity of **X** was also recyclable when Zn^{2+} (10 equiv.) and PPi (10 equiv.) were added in sequence. After two cycles, **X** still showed an ideal response toward the target ions.

In a short, the free **X** showed a weak fluorescence intensity in the ethanol solution. The fluorescence signal was significantly enhanced in the presence of Zn^{2+} and then disappeared when PPi was added to the system, displaying an efficient “on-off-on” fluorescence behavior. These results indicated that **X** could be used as sensor for sequential detection of Zn^{2+} and PPi in acetonitrile buffer solution.

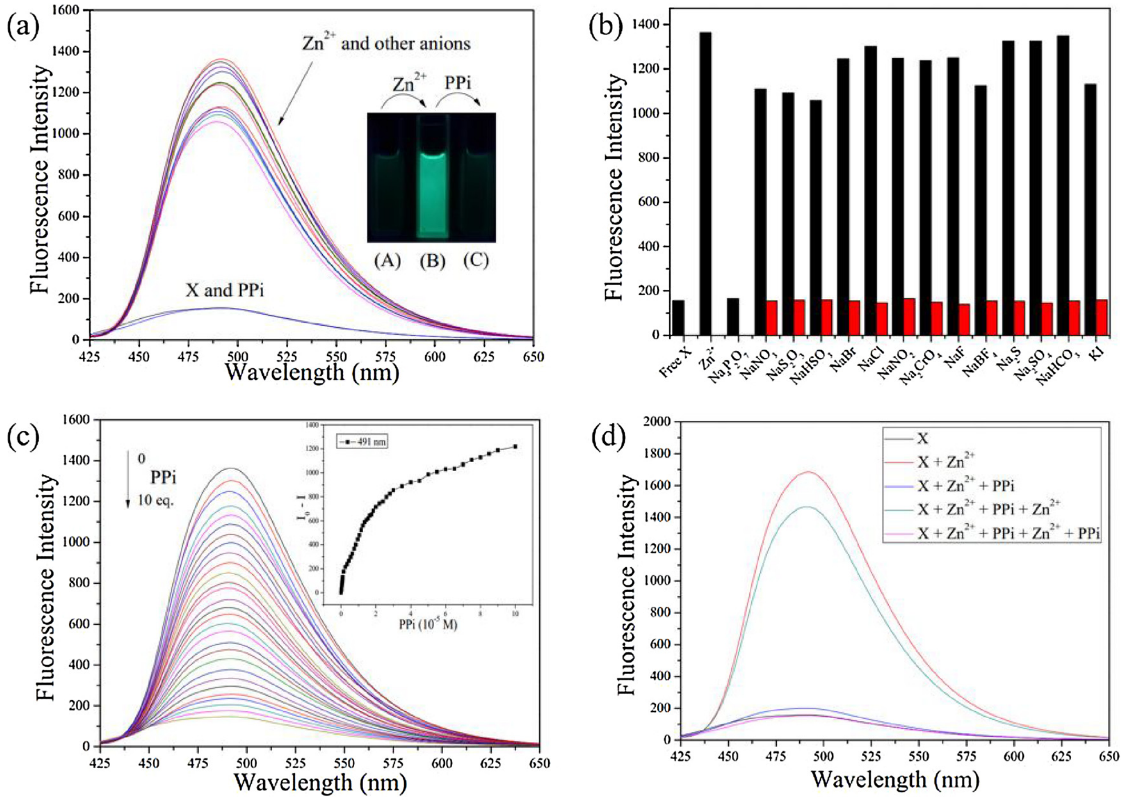

Fig. 3. (a) Fluorescence spectral changes of **X**[Zn^{2+}] upon the addition of various anions ($Na_4P_2O_7$, $NaNO_3$, NaS_2O_3, $NaHSO_3$, NaBr, NaCl, $NaNO_2$, Na_2CrO_4, NaF, $NaBF_4$, Na_2S, Na_2SO_4, $NaHCO_3$ and KI) in acetonitrile/buffer solution (v/v = 9/1, tris =10 mM, pH = 7.4). inset: the color of **X** and **X**[Zn^{2+}] system under a UV lamp. (b) The influence of single anions to the interaction between **X**[Zn^{2+}] and PPi. (c) Fluorescence titration spectral of **X**[Zn^{2+}] upon the addition of different concentrations of PPi. Inset: the change of fluorescence intensity of **X** with the addition of PPi. (d) Reversible switching of the fluorescence intensity of **X** by repeated addition of Zn^{2+} and PPi.

*3.2. The spectroscopic studies of **X** toward In^{3+} in DMF buffer solution*

The fluorescence sensing properties of **X** toward various metal ions (In^{3+}, Cr^{3+}, Ni^{2+}, Ag^{+}, Mg^{2+}, Hg^{2+}, Al^{3+}, Fe^{3+}, Cu^{2+}, Ga^{3+}, Co^{2+}, Cd^{2+}, Mn^{2+}, Li^{2+}, K^{+} and Zn^{2+}) were also investigated in DMF/buffer solution (v/v = 9/1, tris =10 mM, pH = 7.4). As shown in Fig. 4(a) and (b), **X** also showed weak fluorescence in DMF buffer solution at the excitation wavelength of 365 nm. When various of metal ions were added to the **X** solution, only In^{3+} could cause a significant change (about 9 times) in fluorescence intensity at 491 nm, corresponding with the fluorescence color change from colorless (Φ = 0.014) to yellow-green (Φ = 0.2), while other metal ions had no effect on fluorescence intensity (Fig. 4(c)). The results indicated that **X** could be used as a sensor for In^{3+} by fluorescent color changed. Under the same condition,

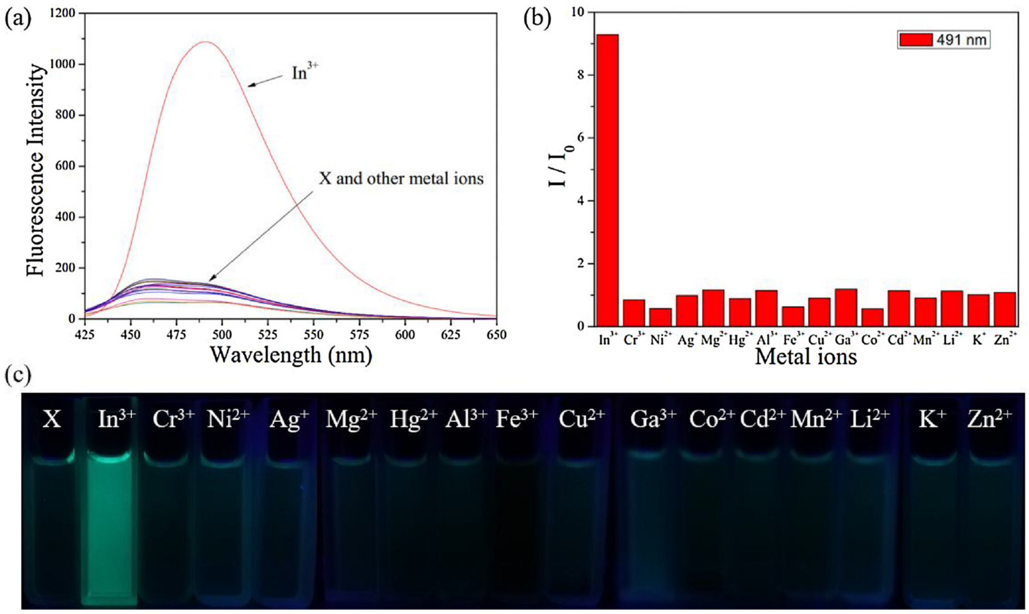

Fig. 4. (a) and (b) Fluorescence spectral changes of **X** (1×10^{-5} M) upon the addition of various metal ions (In^{3+}, Cr^{3+}, Ni^{2+}, Ag^{+}, Mg^{2+}, Hg^{2+}, Al^{3+}, Fe^{3+}, Cu^{2+}, Ga^{3+}, Co^{2+}, Cd^{2+}, Mn^{2+}, Li^{2+}, K^{+}, and Zn^{2+}) in DMF/buffer solution (v/v = 9/1, tris =10 mM, pH = 7.4). (c) Fluorescence pictures of a solution of **X** in the presence of various metal ions under UV light.

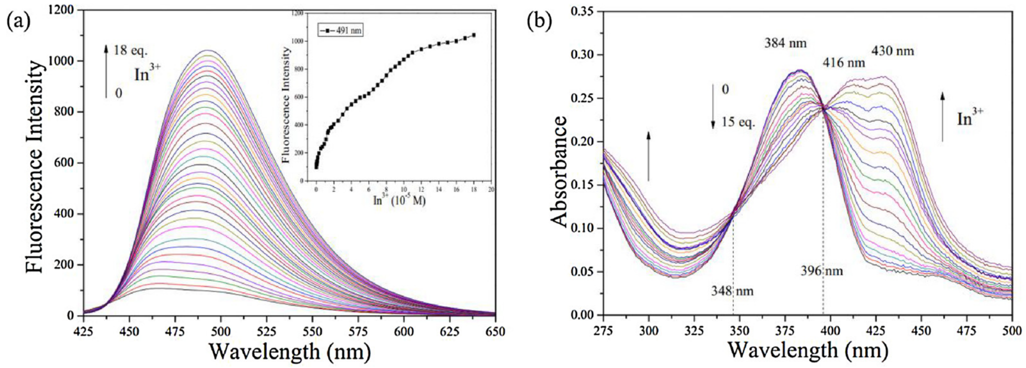

Fig. 5. (a) and (b) Fluorescence and absorption titration spectral of **X** (1×10^{-5} M) upon the addition of different concentrations of In^{3+} in DMF/buffer solution (v/v = 9/1, tris =10 mM, pH = 7.4). Fig. 5(a) inset: the change of fluorescence intensity of **X** with the addition of In^{3+}.

the UV–vis spectral studies of **X** toward various metal ions were also shown in Fig. S13, proving **X** exhibited no or tiny spectral change with addition of most metal ions. However, upon addition of Fe^{3+} Cr^{3+} and Mn^{2+}, the main peak at 384 nm was enhanced. Moreover, upon mixing with In^{3+}, Co^{2+}, Cu^{2+} and Ni^{2+} the original main peak at 384 nm was substituted by the new peak around 430 nm, indicating that they could form complex with **X**. Furthermore, competition experiments were also studied in Fig. S14. In the presence of most metal ions, **X** could still be used as a sensor to detect In^{3+}. These results indicated that **X** had great selectivity for In^{3+} over other metal ions in DMF buffer solution.

Subsequently, to further explore the sensing properties of **X** toward In^{3+}, the fluorescence and absorption titration spectral were explored respectively in DMF/buffer solution (v/v = 9/1, tris =10 mM, pH = 7.4). As shown in Fig. 5(a), with gradual addition of In^{3+} from 0 to 18 equiv. to the solution of **X**, the original weak fluorescence intensity was increased at 491 nm and reached a platform (Fig. 5(a) inset). And as shown in Fig. 5(b), upon with increasing concentration of In^{3+} from 0 to 15 equiv., the original absorption peak decreased gradually at 384 nm along with two new peaks at 416 nm and 430 nm increased steadily. There were two clear isosbestic points at 348 nm and 396 nm, indicating that the **X** form stable complexes (**X**[In^{3+}]) with In^{3+}. In addition, a good linear relationship (R^2 = 0.9877) between the fluorescence intensity of **X** and the concentration of In^{3+} in the range from 0 to 1×10^{-6} M (Fig. S15). The ratio of 1 / (I - I$_0$) also displayed a good linear relationship (R^2 = 0.9870) versus 1 / In^{3+} (Fig. S16). On the basis of experimental data, the detection limit of **X** for In^{3+} and the association constant between **X** and In^{3+} were calculated to be 2.9×10^{-8} M and 2.4×10^4 M^{-1}, respectively, based on the formula LOD = 3σ/s and the Benesi-Hildebrand eqn (2).

The effect of pH on **X** performance was treated in the pH range 2–11. As shown in Fig. S17, the fluorescence intensity of **X** was stable in the pH range of 2–11. Furthermore, in the presence of In^{3+} (15 equiv.), the fluorescence intensity of **X** was enhanced in the pH range of 6–8. Too much acidity (pH < 5) or alkalinity (pH > 10) will affect the recognition of In^{3+} by **X**. Obviously, **X** showed an excellent ability to detection of In^{3+} at pH = 7.4, indicating that **X** had potential for biological testing.

The reversibility test was also carried out in Fig. S18 by adding In^{3+} (15 equiv.) and EDTA (15 equiv.) to the solution of **X** in sequence. The solution of **X** was treated with In^{3+}, leading to a noticeable fluorescence increased. And then, the fluorescence intensity was recovered when EDTA was added into the above solution. In^{3+} and EDTA were sequentially added to the solution of **X** for 4 times with a negligible loss of fluorescence intensity. After 4 cycles, the fluorescence intensity of **X** was still obviously enhanced when upon the addition of In^{3+}.

These results indicated that **X** could also be used as a reversible sensor with high sensitivity and selectivity for detection of Zn^{2+} in DMF buffer solution.

3.3. The binding mechanisms and theoretical calculations

In order to further explore the sensing mechanism between **X** and metal ions (Zn^{2+} and In^{3+}), the binding model between **X** and metal ions (Zn^{2+} and In^{3+}) was proposed based on mass spectrometry titration experiment, which was verified and discussed by Gaussian calculation.

As shown in Fig. S19 and Fig. S20, the peak at *m/z* = 444.06 corresponded to [**X** + Zn^{2+} - H$^+$]$^+$ and the peak at *m/z* = 495.015 corresponded to [**X** + In^{3+} - H$^+$]$^{2+}$, respectively. ESI-mass spectrometry analysis proved the complexation ratio between **X** and metal ions

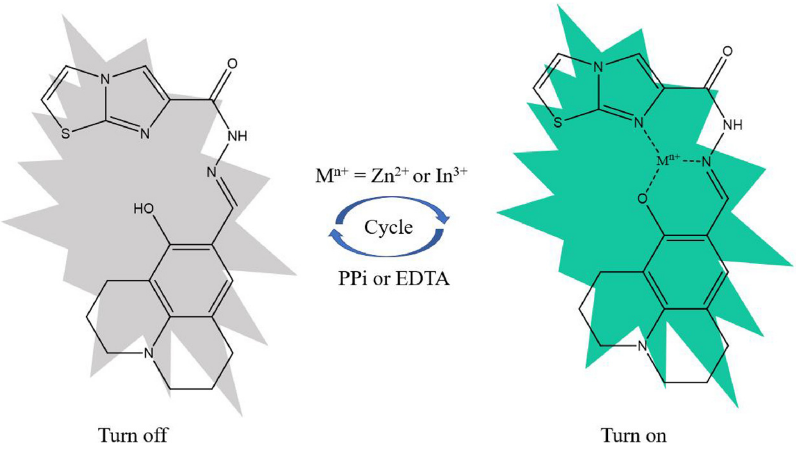

Scheme 2. The proposed binding mode of **X**, **X**[Zn^{2+}] and **X**[In^{3+}].

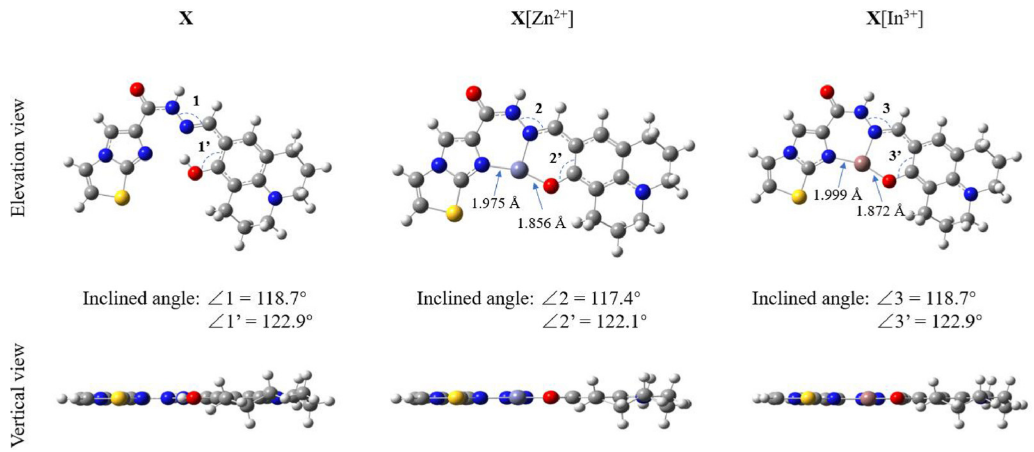

Fig. 6. The optimized geometry of **X** **X**[Zn^{2+}]and **X**[In^{3+}] at the B3LYP level of theory, where the light-gray, red, blue, white, dark-gray, brown and cyan spheres denote C, O, N, H, Zn, In and Cl atoms, respectively.

(Zn^{2+} and In^{3+}) was 1:1. Therefore, based on the results of ESI-mass and relevant literature [53], the possible binding model of **X** and metal ions was proposed in scheme 2 . Obviously, the oxygen atom on the hydroxyl group and the nitrogen atoms on the imidazole ring and the C═N bond were involved in the complexation. After binding with metal ions, the whole molecule (**X**[Zn^{2+}] and **X**[In^{3+}]) may became more stable because it forms two new ring structures.

Subsequently, in order to prove that the binding mechanism between **X** and metal ions was feasible, the molecular structures of **X**, **X**[Zn^{2+}] and **X**[In^{3+}] were calculated and analyzed using the Gaussian 09 program with the B3LYP/6-31 G(d) and B3LYP/LanL2DZ basis set, including structural optimization and energy calculation [53]. The optimized geometry of **X** **X**[Zn^{2+}]and **X**[In^{3+}] were shown in Fig. 6. From the vertical view, it is clear that all three molecules have strong planarity regardless of the presence or absence of metal ions. After binding to metal ions, several key bond angles and bond lengths barely changed, suggesting that **X** could be perfectly bound to metal ions without too much structural modification. As shown in Fig. 7, to further understand the electronic transitions of **X** **X**[Zn^{2+}] and **X**[In^{3+}], the energy calculations of orbital were executed at the optimized molecular structure, including the highest occupied molecular orbital (HOMO) and the lowest unoccupied molecular orbital (LUMO). For free **X**, the HOMO and LUMO were respectively distributed on the julolidine moiety and imidazo[2,1-b]thiazole, indicating that electrons will transfer when excited. So, the weak fluorescence intensity of **X** is due to the photoinduced electron transfer (PET) mechanism. After binding with Zn^{2+} (**X**[Zn^{2+}]), the degree of intramolecular charge was increased, indicating that the corresponding mechanism of **X** on Zn^{2+} was the chelation enhanced fluorescence (CHEF) mechanism. For **X** [In^{3+}], it is clearly observed that both the nitrogen on the imidazole ring and the oxygen on the hydroxyl group had a significant amount of LUMO coefficient with maximum coefficient remaining with In^{3+}. After binding with In^{3+}, the optical transfer of lone pair electrons inside the molecule was prevented, which is the reason for enhanced fluorescence [54]. Moreover, the energy gap of **X** **X**[Zn^{2+}] and **X**[In^{3+}] were also calculated to be 3.63 eV, 2.91 eV and 1.97 eV, respectively. Thus, these results indicated that **X** could from stable complex with Zn^{2+} and In^{3+} ions. The calculated results and experimental phenomena were highly consistent with the theoretical calculation.

3.4. Application of X in real water sample

The **X** was applied to recognition of Zn^{2+}, PPi and In^{3+} in tap water samples. Various concentrations of Zn^{2+}, PPi and In^{3+} were prepared in tap water and were measured by the fluorescence assay method. As shown in Table 1, the satisfactory recovery rate (90.1 %–97.6 %) and RSD (0.86–3.09) were obtained from these samples. Thus, these data indicated that **X** could be used as a sensor for the quantitative detection of Zn^{3+}, PPi and In^{3+} in real water samples.

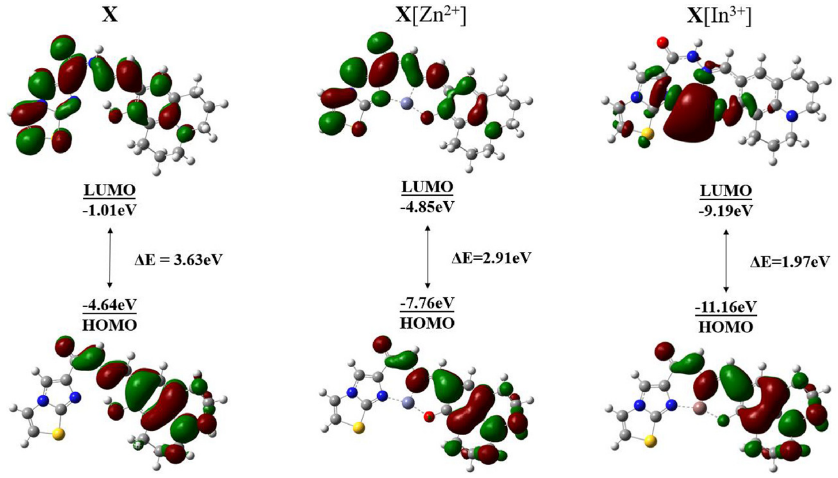

Fig. 7. The energy diagram of HOMO and LUMO orbital of **X** **X**[Zn^{2+}]and **X**[In^{3+}].

Table 1
detection toward Zn^{2+}, PPi and In^{3+} in tap water samples.

Ions	Sample	Ions added (M)	Ions recovered (M)	Recovery (%)	RSD (%)
Zn^{2+}	1	1×10^{-5} M	9.28×10^{-6} M	92.8	3.09
	2	3×10^{-5} M	2.80×10^{-5} M	93.3	1.59
	3	5×10^{-5} M	4.88×10^{-5} M	97.6	2.58
PPi	1	1×10^{-5} M	9.11×10^{-6} M	91.1	1.98
	2	3×10^{-5} M	2.85×10^{-5} M	94.8	2.08
In^{3+}	1	1×10^{-5} M	9.01×10^{-6} M	90.1	1.12
	2	5×10^{-5} M	4.79×10^{-5} M	95.8	0.86

4. Conclusions

In summary, A simple multifunctional sensor, **X**, was designed and synthesized based on 8-hydroxy-2,3,6,7-tetrahydro-1H,5H-pyrido[3,2,1-ij]quinoline-9-carbaldehyde and imidazo[2,1-b]thiazole. The structure of **X** was characterized by NMR, FTIR and ESI-MS spectroscopy. **X** could sequentially identify Zn^{2+} and PPi in acetonitrile buffer solution through the presence or absence of fluorescent signals and could detect In^{3+} in DMF buffer solution with obvious fluorescence enhancement, displaying an efficient “off-on-off” fluorescence behavior. The detection limit for Zn^{2+}, PPi and In^{3+} were calculated to be 4.58×10^{-8} M, 1.07×10^{-8} M and 2.9×10^{-8} M, respectively. Moreover, **X** could quantitatively detect Zn^{2+}, PPi and In^{3+} in real water samples with the satisfactory recovery rate and RSD. In addition, the complexation ratio between **X** and metal ions (Zn^{2+} and In^{3+}) was 1:1. The binding mode and sensing mechanism of X to metal ions (Zn^{2+} and In^{3+}) were verified by Gaussian calculation based on B3LYP/6-31 G(d) and B3LYP/LanL2DZ basis set.

Author statement

Yuankang Xu is studying for master degree in Department of Chemistry at University of Jinan. She received her BS in chemistry at University of Jinan in 2016.

Shufang Yuan is an employee of Henan Sanmenxia Aoke Chemical Industry Co. Ltd.

Yanxia Zhang is a teacher in Department of Chemical Engineering, University of Jinan, China.

Hanyu Wang is studying for master degree in Department of Chemistry at University of Jinan.

Xiaofeng Yang is an associate professor in Department of Chemical Engineering, University of Jinan, China. She received his Ph.D. degree in 2009 from Saitama University, her research focus is chemosensor based on small molecules.

Meishan Pei received his PhD degree in 2000 from Chinese Academy of Sciences. He is a professor in Department of Chemistry and Physics of Polymers. His current research focuses on functional polymer science.

Guangyou Zhang received his PhD degree in 1993 from Nanjing Forestry University. He is a professor in Department of Chemical Engineering, University of Jinan, China. His current research interests are mainly in the development of sensors for surfactants, metal ions, pharmaceutical anions, proteins and DNA based on fluorescent molecules.

All authors contribute equally.

Declaration of Competing Interest

The authors declare no conflict of interest.

Acknowledgements

The authors thank the Henan Sanmenxia Aoke Chemical Industry Co., Ltd. w0920 for financial support. Financial support by the National Natural Science Foundation of China Grants 21708013 and the China Postdoctoral Science Foundation Grants 2017M620288

Appendix A. Supplementary data

Supplementary material related to this article can be found, in the online version, at doi:https://doi.org/10.1016/j.jphotochem.2019.112348.

References

[1] N. Behera, V. Manivannan, A probe for multi detection of Al^{3+}, Zn^{2+} and Cd^{2+} ions via turn-on fluorescence responses, J. Photochem. Photobiol. A: Chem. 353 (2018) 77–85.

[2] W. Zhu, X. Huang, Z. Guo, X. Wu, H. Yu, Tian He, A novel NIR fluorescent turn-on sensor for the detection of pyrophosphate anion in complete water system, Chem. Commun. 48 (2012) 1784–1786.

[3] T.G. Jo, K.H. Bok, J. Han, M.H. Lim, C. Kim, Colorimetric detection of Fe^{3+} and Fe^{2+} and sequential fluorescent detection of Al^{3+} and pyrophosphate by an imidazole-based chemosensor in a near-perfect aqueous solution, Dye. Pigment. 139 (2017) 136–147.

[4] X.J. Bai, J. Ren, J. Zhou, Z.B. Song, A ‘turn-on’ fluorescent chemosensor for the detection of Zn^{2+} ion based on 2-(quinolin-2-yl) quinazolin-4(3*H*)-one, Heterocycl. Commun. 24 (2018) 135–139.

[5] Y.P. Zhang, Q.H. Xue, Y.S. Yang, X.Y. Liu, C.M. Ma, J.X. Ru, H.C. Guo, A chromene pyrazoline derivatives fluorescent probe for Zn^{2+} detection in aqueous solution and living cells, Inorganica Chim. Acta 479 (2018) 128–134.

[6] M. Formica, G. Favi, V. Fusi, L. Giorgi, F. Mantellini, M. Micheloni, Synthesis and study of three hydroxypyrazole-based ligands: a ratiometric fluorescent sensor for Zn(II), J. Lumin. 195 (2018) 193–200.

[7] H. Wang, T. Kang, X. Wang, L. Feng, A facile strategy for achieving high selective Zn (II) fluorescence probe by regulating the solvent polarity, Talanta 184 (2018) 7–14.

[8] Y. Tang, Y. Huang, L. Lu, C. Wang, T. Sun, J. Zhu, G. Zhu, J. Pan, Y. Jin, A. Liu, M. Wang, Synthesis of a new pyrene-devived fluorescent probe for the detection of Zn^{2+}, Tetrahedron Lett. 59 (2018) 3916–3922.

[9] M.J. Chang, M.H. Lee, A highly selective dual-channel fluorescent probe for the detection of Zn^{2+} ion and pyrophosphate in micelle, Dye. Pigment. 149 (2018) 915–920.

[10] H. Liu, Y. Tan, Q. Dai, H. Liang, J. Song, J. Qu, W.Y. Wong, A simple amide fluorescent sensor based on quinoline for selective and sensitive recognition of zinc (II) ions and bioimaging in living cells, Dye. Pigment. 158 (2018) 312–318.

[11] H.J. Jang, J.H. Kang, D. Yun, C. Kim, A multifunctional selective “turn-on” fluorescent chemosensor for detection of Group IIIA ions Al^{3+}, Ga^{3+} and In^{3+}, Photochem. Photobiol. Sci. 17 (2018) 1247–1255.

[12] A. Kim, J.H. Kang, H.J. Jang, C. Kim, Fluorescent detection of Zn(II) and In(III) and colorimetric detection of Cu(II) and Co(II) by a versatile chemosensor, J. Ind. Eng. Chem. 65 (2018) 290–299.

[13] Y.C. Wu, H.J. Li, H.Z. Yang, A sensitive and highly selective fluorescent sensor for In^{3+}, Org. Biomol. Chem. 8 (2010) 3394–3397.

[14] H. Cho, J.B. Chae, C. Kim, A thiophene-based blue-fluorescent emitting chemosensor for detecting indium (III) ion, Inorg. Chem. Commun. 97 (2018) 171–175.

[15] L.M. Mesquita, V. Andre, C.V. Esteves, T. Palmeira, M.N. Berberan-Santos, P. Mateus, R. Delgado, Dinuclear Zinc(II) macrocyclic complex as receptor for selective fluorescence sensing of pyrophosphate, Inorg. Chem. 55 (2016) 2212–2219.

[16] X. Feng, Y. An, Z. Yao, C. Li, G. Shi, A turn-on fluorescent sensor for pyrophosphate based on the disassembly of Cu^{2+}-mediated perylene diimide aggregates, ACS Appl. Mater. Interfaces 4 (2012) 614–618.

[17] A.K. Mahapatra, S.K. Manna, C.D. Mukhopadhyay, D. Mandal, Pyrophosphate-selective fluorescent chemosensor based on ratiometric tripodal-Zn(II) complex: Application in logic gates and living cells, Sens. Actuators B Chem. 200 (2014) 123–131.

[18] J.H. Kang, J. Han, H. Lee, M.H. Lim, K.T. Kim, C. Kim, A water-soluble fluorescence chemosensor for the sequential detection of Zn^{2+} and pyrophosphate in living cells and zebrafish, Dye. Pigment. 152 (2018) 131–138.

[19] R.R. Zhao, Q.L. Xu, Y. Yang, J. Cao, Y. Zhou, R. Xu, J.F. Zhang, A coumarin-based terpyridine–zinc complex for sensing pyrophosphate and its application in in vivo imaging, Tetrahedron Lett. 57 (2016) 5022–5025.

[20] N. Roy, H.A.R. Pramanik, P.C. Paul, S.T. Singh, A sensitive schiff-base fluorescent chemosensor for the selective detection of Zn^{2+}, J. Fluoresc. 24 (2014) 1099–1106.

[21] T.A. Khan, M. Sheoran, S. Jain, D. Gupta, S.G. Naik, Screening of biologically important Zn^{2+} by a chemosensor with fluorescent turn on-off mechanism, Spectrochimica Acta Part A: Mol. 189 (2018) 176–182.

[22] Y. Liu, Y. Li, Q. Feng, N. Li, K. Li, H. Hou, B. Zhang, ‘Turn-on’ fluorescent chemosensors based on naphthaldehyde-2-pyridinehydrazone compounds for the detection of zinc ion in water at neutral pH, Luminescence 33 (2018) 29–33.

[23] J. Zhu, Y. Zhang, Y. Chen, T. Sun, Y. Tang, Y. Huang, Q. Yang, D. Ma, Y. Wang, M. Wang, A Schiff base fluorescence probe for highly selective turn-on recognition of Zn^{2+}, Tetrahedron Lett. 58 (2017) 365–370.

[24] L. Tang, X. Dai, K. Zhong, D. Wu, X. Wen, A novel 2,5-diphenyl-1,3,4-oxadiazole derived fluorescent sensor for highly selective and ratiometric recognition of Zn^{2+} in water through switching on ESIPT, Sens. Actuators B Chem. 203 (2014) 557–564.

[25] J. Hu, J. Li, J. Qi, Y. Sun, Acylhydrazone based fluorescent chemosensor for zinc in

aqueous solution with high selectivity and sensitivity, Sens. Actuators B Chem. 208 (2015) 581–587.

[26] T. Xu, H. Duan, X. Wang, X. Meng, J. Bu, Fluorescence sensors for Zn^{2+} based on conjugated indole Schiff base, Spectrochimica Acta Part A: Mol. 138 (2015) 603–608.

[27] Z. Wang, S. Cui, S. Qiu, Z. Zhang, S. Pu, A highly sensitive fluorescent sensor for Zn^{2+} based on diarylethene with an imidazole unit, Spectrochimica Acta Part A: Mol. 205 (2018) 21–28.

[28] S. Pratibha, S. Singh, Sivakumar, S. Verma, Purine-based fluorescent sensors for imaging zinc ions in HeLa cells, Eur. J. Inorg. Chem. (2017) 4202–4209.

[29] L. Subha, C. Balakrishnan, S. Natarajan, M. Theetharappan, B. Subramanian, M.A. Neelakantan, Water soluble and efficient amino acid Schiff base receptor for reversible fluorescence turn-on detection of Zn^{2+} ions: quantum chemical calculations and detection of bacteria, Spectrochimica Acta Part A: Mol. 153 (2016) 249–256.

[30] K. Aich, S. Goswami, S. Das, C.D. Mukhopadhyay, A new ICT and CHEF based visible light excitable fluorescent probe easily detects in vivo Zn^{2+}, RSC Adv. 5 (2015) 31189–31194.

[31] Y. Fu, C. Fan, G. Liu, S. Cui, S. Pu, A highly selective and sensitive ratiometric fluorescent chemosensor for Zn^{2+} based on diarylethene with a benzyl-linked 8-aminoquinoline-2-aminomethylpyridine unit, Dye. Pigment. 126 (2016) 121–130.

[32] X. Tian, X. Guo, L. Jia, Y. Zhang, Bi-8-carboxamidoquinoline derivatives for the fluorescent recognition of Zn^{2+}, J. Fluoresc. 25 (2015) 441–449.

[33] Z. Kowser, U. Rayhan, S. Rahman, P.E. Georghiou, T. Yamato, A fluorescence "turn-on" sensor for multiple analytes: OAc^- and F^- triggered fluorogenic detection of Zn^{2+} in a co-operative fashion, Tetrahedron 73 (2017) 5418–5424.

[34] J. Jung, A. Dinescu, Emission pathway switching by solvent polarity: Facile synthesis of benzofuran-bipyridine derivatives and turn-on fluorescence probe for zinc ions, Tetrahedron Lett. 58 (2017) 358–361.

[35] Y. Guo, L. Wang, J. Zhuo, B. Xu, X. Li, J. Zhang, Z. Zhang, H. Chi, Y. Dong, G. Lu, A pyrene-based dual chemosensor for colorimetric detection of Cu^{2+} and fluorescent detection of Fe^{3+}, Tetrahedron Lett. 58 (2017) 3951–3956.

[36] A. Jiménez-Sánchez, B. Ortiz, V.O. Navarrete, J.C. Flores, N. Farfán, R. Santillan, A dual-model fluorescent Zn^{2+}/Cu^{2+} ions sensor with in-situ detection of $S^{2-}/(PO_4)$-and colorimetric detection of Fe^{2+} ion, Inorganica Chim. Acta 429 (2015) 243–251.

[37] T. Anand, A.K.SK, S.K. Sahoo, V.B. Cofactor Derivative, A dual fluorescent turn-on sensor to detect Zn^{2+} and CN ions and its application in live cell imaging, ChemistrySelect 2 (2017) 7570–7579.

[38] J. Qin, Z. Yang, Design of a novel coumarin-based multifunctional fluorescent probe for $Zn^{2+}/Cu^{2+}/S^{2-}$ in aqueous solution, Mater. Sci. Eng. C 57 (2015) 265–271.

[39] F. Liu, C. Fan, Y. Tu, S. Pu, A new fluorescent and colorimetric chemosensor for Al^{3+} and F^-/CN^- based on a julolidine unit and its bioimaging in living cells, RSC Adv. 8 (2018) 31113–31120.

[40] Y.W. Choi, J.J. Lee, E. Nam, M.H. Lim, C. Kim, A fluorescent chemosensor for Al^{3+} based on julolidine and tryptophan moieties, Tetrahedron 72 (2016) 1998–2005.

[41] D.H. Joo, J.S. Mok, G.H. Bae, S.E. Oh, J.H. Kang, C. Kim, Colorimetric detection of Cu^{2+} and fluorescent detection of $PO_4{}^{3-}$ and S^{2-} by a multifunctional chemosensor, Ind. Eng. Chem. Res. 56 (2017) 8399–8407.

[42] Y.W. Choi, G.R. You, J.J. Lee, C. Kim, Turn-on fluorescent chemosensor for selective detection of Zn^{2+} in an aqueous solution: Experimental and theoretical studies, Inorg. Chem. Commun. 63 (2016) 35–38.

[43] Y.Q. Gu, W.Y. Shen, Y. Zhou, S.F. Chen, Y. Mi, B.F. Long, D.J. Young, F.L. Hu, A pyrazolopyrimidine based fluorescent probe for the detection of Cu^{2+} and Ni^{2+} and its application in living cells, Spectrochimica Acta Part A: Mol. 209 (2019) 141–149.

[44] L.Y. Qin, L.J. Hou, J. Feng, J.B. Chao, Y. Wang, W.J. Jin, A reversible turn-on colorimetric and fluorescent sensor for Al^{3+} in fully aqueous media and its living cell imaging, Synth. Met. 221 (2016) 206–213.

[45] L. Fan, J. Qin, T. Li, B. Wang, Z. Yang, A novel rhodamine chromone-based "Off-On" chemosensor for the differential detection of Al(III) and Zn(II) in aqueous solutions, Sens. Actuators B Chem. 203 (2014) 550–556.

[46] D. Singhal, N. Gupta, A.K. Singh, Fluorescent sensor for Al^{3+} ion in partially aqueous media using julolidine based probe, New J. Chem. 40 (2016) 7536–7541.

[47] J. Sun, Z. Liu, Y. Wang, S. Xiao, M. Pei, X. Zhao, G. Zhang, A fluorescence chemosensor based on imidazo[1,2-a]quinoline for Al^{3+} and Zn^{2+} in respective solutions, RSC Adv. 5 (2015) 100873–100878.

[48] Y. Xu, H. Wang, J. Zhao, X. Yang, M. Pei, G. Zhang, Y. Zhang, L. Lin, A simple fluorescent schiff ; base for sequential detection of Zn^{2+} and PPi based on imidazo [2,1-*b*]thiazole, J. Photochem. Photobiol. A: Chem. 383 (2019) 112026.

[49] J.A. Kaizerman, M.I. Gross, Y. Ge, S. White, W. Hu, J. Duan, E.E. Baird, K.W. Johnson, R.D. Tanaka, H.E. Moser, R.W. Burli, DNA binding ligands targeting drug-resistant Bacteria: structure, activity, and pharmacology, J. Med. Chem. 46 (2003) 3914–3929.

[50] F. XXXX, A. Ali, R. Guo, J. Tian, H. Wang, Z. Li, D. Zhang, Methionine-derived Schiff base as selective fluorescent "turn-on" chemosensor for Zn^{2+} in aqueous medium and its application in living cells imaging, Sens. Actuators B Chem. 211 (2015) 544–550.

[51] J.J. Lee, S.A. Lee, H. Kim, L. Nguyen, I. Noh, C. Kim, A highly selective CHEF-type chemosensor for monitoring Zn^{2+} in aqueous solution and living cells, RSC Adv. 5 (2015) 41905–41913.

[52] G.R.C. Hamilton, Y. Sheng, B. Callan, R.F. Donnelly, J.F. Callan, A hydrogel based zinc(II) sensor for use in fluorescent multi-well plate analysis, New J. Chem. 39 (2015) 3461–3466.

[53] Y. Xu, H. Wang, J. Zhao, X. Yang, M. Pei, G. Zhang, Y. Zhang, A dual functional fluorescent sensor for the detection of Al^{3+} and Zn^{2+} in different solvents, New J. Chem. 43 (2019) 14320–14326.

[54] U. Ghosh, S. Sekhar Bag, C. Mukherjee, Bis-pyridobenzene as a fluorescence light-up sensor for Hg^{2+} Ion in water, Sens. Actuators B Chem. 238 (2017) 903–907.